Accepted for publication in Journal of Wind Engineering and Industrial Aerodynamics

Moisture response of building facades to wind-driven rain: field measurements compared with numerical simulations

M. Abuku [a, *], B. Blocken [b], S. Roels [a]

[a] *Laboratory of Building Physics, Department of Civil Engineering, Katholieke Universiteit Leuven, Kasteelpark Arenberg 40, 3001 Leuven, Belgium*
[b] *Building Physics and Systems, Eindhoven University of Technology, P.O. Box 513, 5600 MB Eindhoven, the Netherlands*
[*] *Corresponding author: Masaru Abuku, Tel: +32 16 321348, Fax: +32 16 321980, e-mail: masaru.abuku@bwk.kuleuven.be*

Abstract

Wind-driven rain (WDR) is one of the most important boundary conditions governing the hygrothermal behaviour of building facades, which is usually numerically analysed with so-called Heat-Air-Moisture (HAM) transfer models. In the traditional approach of HAM transfer models, WDR is implemented in a simplified manner: the total mass of all raindrops impinging on a certain surface area of a building facade during the time interval of the meteorological input data (typically one hour) is spatially and temporally averaged and is supplied to the facade as an averaged moisture flux. However, real WDR is the sum of individual raindrops that impinge on the facade in a spatially and temporally discrete modus, and that do not only spread at impact, but may also splash or bounce off the facade. Therefore the reliability of this simplification can be questioned. To investigate its validity, a new experimental set-up was developed at a full-scale test building. It allows simultaneous and continuous measurements of the reference wind speed and direction, WDR intensity, outdoor air temperature and humidity as well as the response of facade material samples to these environmental conditions. For this purpose, a measuring device was developed that monitors the weight change of the sample with a resolution of 5 mg. Temperatures at the interior and exterior material surfaces are also monitored. The whole measurement data set is used to check the validity of the traditional numerical approach. Large differences are found between the measurement and simulation results, which cannot solely be attributed to the uncertainty in the convective moisture transfer coefficient, but may be due to two additional reasons: the occurrence of splashing and bouncing at raindrop impact on the facade, which is not included in the model, and/or errors in surface moisture evaporation and absorption due to modelling the actual random and discrete raindrop impingement as a simplified averaged moisture flux.

Keywords: driving rain; moisture transfer; HAM analysis; convective moisture transfer coefficient; on site experiment; water drop impact; rainwater uptake; numerical simulation; validation

Nomenclature

A	water absorption coefficient (kg/m^{2}s$^{0.5}$)
d	raindrop diameter (mm)
g_m	moisture flux (kg/m^{2}s)
I_{WDR}	wind-driven rain intensity on a building facade (mm/h)
m	weight change of a specimen (g)
p	vapour pressure (Pa)
S_{WDR}	cumulative amount of wind-driven rain (mm)
U_{10}	reference wind speed at 10 m above the ground (m/s)
w_c	capillary moisture content (kg/m^3)
Greek letters	
β	convective moisture transfer coefficient (s/m)
Δm	material weight change in one hour (g)
ΔS_{WDR}	wind-driven rain sum in one hour (g)
ϕ	impact angle (º)
φ_{10}	reference wind direction at 10 m above the ground (º from N)
θ	temperature (ºC)

Subscripts

e	external
sem	semi-empirical
exa	exact
mea	measured
s	surface
sat	saturated
sim	simulated

Acronyms

CFD	computational fluid dynamics
HAM	heat-air-moisture
NMR	nuclear magnetic resonance
PMMA	polymethyl-methacrylate
PVC	polyvinyl-chloride
WDR	wind-driven rain

1. Introduction

Wind-driven rain (WDR) is the result of the interaction of airflow and rainfall. It is one of the most important moisture sources governing the hygrothermal behaviour of building facades and thus of great concern in the field of building physics (Choi, 1994a, 1999; Sanders, 1996; Künzel and Kiessl, 1997; Lacasse, 2003; Blocken and Carmeliet, 2004; Abuku et al., 2009c). The research of WDR in this field comprises two consecutive steps: (1) the determination of WDR loads on building facades and (2) the determination of the response of walls to WDR loads. This second step could be subdivided into two parts: (2a) the determination of the response of building components that consist of material layers that are considered isotropic and homogeneous; and (2b) the determination of the response of building components that consist of material layers that are not isotropic and/or not homogenous. Examples of the latter part include masonry and all other building components with cracks and joints. In this paper, we only focus on part (2a). The reason is that the bulk of numerical modelling efforts in the past has concentrated on (2a) (e.g. Hall and Kalimeris, 1982, 1984; Künzel and Kiessl, 1997; Karagiozis et al., 2003; Hagentoft et al., 2004; Straube and Schumacher, 2006; Blocken et al., 2007; Janssen et al. 2007a, 2007b). Therefore, the term “step 2” will refer to part “2a”. Apart from measurements and semi-empirical models in the first step (e.g. Sanders, 1996; Blocken and Carmeliet, 2004), numerical models have been developed in both steps (1) and (2a). Given the complexity of WDR and its importance as a moisture source for building components, the validation of these numerical models, especially via full-scale measurements, is imperative (Dalgliesh and Surry, 2003). While several researchers investigated the validity of the numerical model developed by Choi (1991, 1993, 1994a, 1994b) and its extension to the time domain by Blocken and Carmeliet (2002) for the first step, significantly less researchers addressed the validity of the traditional way in which WDR is implemented in so-called Heat-Air-Moisture (HAM) transfer models for porous building components (second step). This paper focuses on the implementation of WDR in HAM models. In the traditional approach of HAM transfer models, WDR is implemented in a simplified manner: the total mass of all raindrops impinging on a certain surface area of a building facade during the time interval of the meteorological input data (typically one hour) is spatially and temporally averaged and is supplied to the facade as an averaged moisture flux. However, real WDR is the sum of individual raindrops that impinge on the facade in a spatially and temporally discrete modus, and that do not only spread at impact on the facade surface, but may also splash or bounce off the facade. Therefore, the reliability of the traditional approach can be questioned. Note that this approach generally does not consider the possibility of splashing and bouncing, and assumes that the total mass of raindrops is available for absorption by the porous facade material.

This paper investigates the validity of the traditional approach under real atmospheric conditions. First, the state-of-the-art in the two steps of WDR research is provided to clarify the position of the current study. Second, the traditional approach is outlined. Third, field measurements of both WDR loads on building facades and the response of walls to these moisture loads are presented. Measurement results are finally compared with simulation results to investigate the validity of the traditional approach.

2. State-of-the-art

Fig. 1 is a schematic overview of recent studies and the scope and focus of the current study in

approaches for both steps. The letters [a] - [l] in Fig. 1 point to the entries in Table 1. As shown in Fig. 1 and Table 1, WDR research to determine WDR loads on building facades (step 1: the upper part of Fig. 1 and Table 1) has been conducted using experimental, semi-empirical or numerical approaches (Choi, 1993; Sanders, 1996; Blocken and Carmeliet, 2004). On the other hand, the moisture response of porous building facades to WDR loads (step 2: the lower part of Fig. 1 and Table 1) is mostly studied via numerical simulation with HAM transfer models. The wind-driven rain intensity ($I_{WDR,mea}$, $I_{WDR,sem}$ and $I_{WDR,sim}$), obtained from one of the three approaches in the first step, is then used as input for HAM (hygrothermal) analyses in the second step. Thus far each research effort in the past, indicated by [a] - [l] in Fig. 1 and summarised in Table 1, was targeted at developing one of the approaches in each step and/or investigating the validity of the approach. The lines in Fig. 1 and the corresponding letter labels visualise research efforts in which different approaches have been compared with each other for investigating the validity.

Although a comprehensive review of the first step was given by Blocken and Carmeliet (2004), a brief overview with emphasis on recent studies is given below to clarify the scope and focus of the current paper in the framework of WDR research. So far, measurements, which are often time consuming, have been reported by several researchers over more than the past half century. The accuracy of measurements strongly depends on the type of WDR gauges (Högberg et al, 1999; Van Mook, 2002). Blocken and Carmeliet (2005, 2006a) showed that errors in measurements can—at least in the climate under consideration—be for a large part attributed to the evaporation of adhesion water at the surfaces of the WDR gauge. When all parameters in semi-empirical formulae and the meteorological data such as wind speed, wind direction and horizontal rainfall intensity are available, so-called semi-empirical methods can facilitate a speedy calculation and thus are practically useful. However the use of this approach should be limited to rough estimates of WDR loads at facades (Blocken and Carmeliet, 2004). Recent advances in Computational Fluid Dynamics (CFD) to predict the airflow around buildings enabled the trajectory of raindrops to be simulated, providing detailed calculation results of WDR loads on building facades (Choi, 1991, 1993, 1994a, 1994b, 1999; Hangan 1999, Blocken and Carmeliet, 2002, 2006b, 2007). So far, the validity of this CFD WDR simulation method has been investigated from various points of view. For example, validations by comparing simulations to field measurements were performed under different conditions (van Mook, 2002; Blocken and Carmeliet, 2002, 2005, 2006b, 2007; Tang and Davidson, 2004; Tang et al., 2004; Abuku et al., 2009a; Briggen et al., 2009) (see [e] in Fig. 1). Also a validation study by comparing simulations to wind tunnel measurements was performed (Hangan, 1999).

In the traditional approach of HAM transfer models (e.g. Hall and Kalimeris, 1982, 1984; Künzel and Kiessl, 1997; Hagentoft et al., 2004 – see [g] in Fig. 1), WDR as a moisture source for building components is imposed at the facade surface as a simplified flux that is spatially averaged over a certain surface area and temporally averaged over the time interval of the meteorological input data (typically one hour). Karagiozis et al. (2003) and Straube and Schumacher (2006) combined HAM models with WDR loads determined by semi-empirical methods ($I_{WDR,sem}$) in order to investigate the response of facades ($m_{sim}(I_{WDR,sem})$) (see [j] in Fig. 1). Recently, Blocken et al. (2007) and Janssen et al. (2007a, 2007b) proposed the use of numerically determined WDR loads $I_{WDR,sim}$, enabling a more detailed spatial and temporal distribution of WDR loads across the facade to be implemented ([k] in Fig. 1). Although the CFD WDR simulation considers individual drops, it does not consider the random raindrop impingement process, and its results are converted to WDR fluxes averaged over a certain surface area and over the time interval of the meteorological input data, and are as such used as input for HAM simulations. It is important to note that Blocken et al. (2007) analysed the influence of the time resolution of the meteorological input data on the HAM simulation results. They found that, for some rain events, using hourly data can lead to large underestimations of surface and average moisture content, and that using e.g., 10-minute data should be preferred.

However, as mentioned before, real WDR is the sum of individual raindrops that impinge on the facade in a temporally and spatially discrete modus. Apart from spreading at impact, they may also splash or bounce off the facade. Let us define $I_{WDR,exa}$ as the real exact WDR load that is supplied onto the facade material and that is available for absorption and/or evaporation. It does not include those fractions of impinging raindrops that are lost due to splashing and/or bouncing at impact. $I_{WDR,exa}$ does not always exactly equal $I_{WDR,mea}$, $I_{WDR,sem}$, or $I_{WDR,sim}$. Regardless of the difference between the model and reality, only little attention has thus far been paid to the reliability of the traditional approach for WDR loads in HAM models. A first step toward understanding such difference was taken by Künzel and Kiessl (1997) by experimentally investigating the moisture response of building facades to WDR loads over 80 days (see [h] in Fig. 1). In this study, moisture content profiles in a building component specimen were

recorded with the Nuclear Magnetic Resonance (NMR) technique with a time interval of one to a few days. The response of the specimen was then numerically analysed with a one-dimensional (1-D) HAM model with the traditional approach for WDR, using $I_{WDR,mea}$ as input (see [i] in Fig. 1). However, in these calculations, $I_{WDR,mea}$ was adjusted using a reduction factor that the authors called "rain absorptivity", to obtain a better agreement between the simulated and measured material weight changes. This global factor was obtained for the entire measurement period (80 days). Künzl and Kiessl (1997) found the rain absorptivity to be 0.7 (-) for the given conditions. Although this coefficient is just a global factor, which can be tuned at will, the result does suggest that traditional HAM analyses can overestimate the moisture content in walls under WDR loads. The next section briefly summarizes the traditional approach to implement WDR in HAM models.

3. The traditional approach to implement wind-driven rain in HAM models and its uncertainty

The traditional approach to implement WDR in HAM models refers to 1-D HAM analyses in which the total mass of all raindrops impinging on a certain surface area of a building facade during the time interval of the meteorological input data (typically one hour) is spatially and temporally averaged into an averaged moisture flux. Without runoff of raindrops/rainwater, the moisture flux at the outside wall surface g_m (kg/m^{2}s) as boundary condition for the heat and moisture transfer equations in building components, can be expressed as (e.g. Blocken et al., 2007; Janssen et al., 2007b):

$$g_m = -\beta_e \left(p_e - p_{s,e} \right) - I_{WDR} \tag{1}$$

where β_e is the outside convective moisture transfer coefficient (s/m), p_e and $p_{s,e}$ are the vapour pressures (Pa) of the outdoor air and at the outside wall surface, respectively, and I_{WDR} is the WDR intensity (kg/m^{2}s) loaded to the outside wall surface. Note that I_{WDR} can be determined by experimental, semi-empirical or numerical means as shown in Fig. 1. This simplified equation is quite tempting for a simple and speedy simulation and thus has been widely applied (e.g. Hall and Kalimeris, 1982, 1984; Künzel and Kiessl, 1997; Hagentoft et al., 2004; Blocken et al., 2007; Janssen et al., 2007a, 2007b). However, its validity is uncertain because of the difference between the model and reality. Accurate and complete measurement data are required to investigate the validity and give physical insights into possible differences between simulated and measured hygrothermal responses of walls.

4. Experimental set-up and measurements

The intention of the new experimental set-up and the measurements presented in this section is to obtain detailed measurements of the moisture response (weight change) of a building material test sample (m_{mea}) and the relevant meteorological parameters to analyse the accuracy of simulations of the moisture response with the traditional approach ($m_{sim}(I_{WDR,mea})$).

4.1. Experimental set-up at test building

To investigate the validity of the traditional approach, a reliable measurement data set is needed. This section describes the set-up developed for this purpose at the VLIET test building (Hens et al., 2003) located at K.U.Leuven, Belgium. The test building itself was constructed for the comprehensive study of the hygrothermal behaviour of building components under "real" climatic conditions. Apart from the building itself, in which the new test set-up is situated, the building is equipped with a meteorological mast and rain gauge in the free field (Blocken and Carmeliet, 2005). With one ultrasonic anemometer at the top of the mast, the wind speed U_{10} and wind direction φ_{10} at 10 m above the ground are recorded, whereas three cup anemometers at the mast measure the wind speeds at 2, 4 and 6 m above the ground. Fig. 2 shows a photograph taken from the south-west direction of the building settled on the field surrounded by some trees and a few low-rise buildings. The mast and rain gauge are placed at a distance of 20 m from the south-west facade of the test building. This distance was determined based on CFD simulations as the minimum distance for which the presence of the building does not influence these measurements for south-west wind direction (Blocken and Carmeliet 2005). Note that, for other wind directions however (e.g., NE), the mast and rain gauge will be in the flow region that is disturbed by the building. Therefore, the study in this paper will focus on south-west wind direction. The location of the test section and the new set-up in the building are also indicated. This building was used earlier for the

validation of CFD simulations of WDR and successful results were shown (Blocken and Carmeliet, 2002, 2005, 2006b, 2007).

The newly developed set-up at the test section is illustrated in Fig. 3. It consists of a device to measure the weight change m_{mea} of the specimen, PMMA WDR gauges on the wall, temperature sensors at the material surfaces, and a collector gauge for the runoff water. Four test subsections (A-D) were constructed inside the wall of the building. In each test subsection a building material specimen can easily be fixed. With the set-up, the moisture response (weight change) and surface temperatures of the specimen, the amount of the runoff water and the WDR intensity next to the specimen are measured simultaneously. The principle of leverage was used in the measuring device of m_{mea} to increase the precision. The proportion of the length of the lever on the specimen side to that on the other side is two and the precision of the balance is 10 mg. Hence any material weight change larger than 5 mg is measurable. For example, if the intensity of the impinging rain is 0.01 mm/h, the total amount of the rain impinging a 0.25 m $\times$ 0.45 m material sample surface for 10 minutes yields 190 mg, while the mass of a raindrop with a diameter of 1 mm is just 0.52 mg. From this estimate, the accuracy of the measuring device is considered to be precise enough to measure m_{mea} of the material samples. To prevent horizontal disturbance by the wind without disturbing the material movement in the vertical direction, a roller supports the material at the back side (see Fig. 3).

4.2. Measurements of wind-driven rain and the response of walls

Fig. 4 shows results of measurements performed during two periods in 2007: November 29, 0:00 (GMT +1:00) - December 2, 0:00 and December 3, 20:00 - December 12, 15:00. In all measurements described in the current paper, a specimen of calcium silicate (0.25 m×0.45 m×0.09 m) was used because its very high capillary moisture content (w_c = 803 kg/m^3) and water absorption coefficient (A = 1.22 kg/m^{2}s$^{0.5}$) (Roels et al., 2004) allow longer-term measurements without surface saturation. Note that at surface saturation, runoff will occur. Calcium silicate is considered homogeneous and isotropic. No joints and visible cracks are present in the specimen. All specimen surfaces except the exterior surface were water and vapour tight sealed and thus were not exposed to any moisture flow. Figs. 4(a) and (b) show the weight change m_{mea} of the specimen from the initial value, the cumulative amount $S_{WDR,mea}$ of the WDR and the WDR intensity $I_{WDR,mea}$. Note that m_{mea} was measured at the test subsection B, whereas $S_{WDR,mea}$ and $I_{WDR,mea}$ were measured at the test subsection A (Fig. 3). No runoff occurred during these measurements. The figures show that m_{mea} increased during WDR and decreased due to evaporation afterwards. Furthermore the temperatures at the centre of the exterior and interior surfaces of the specimen and the outdoor air temperature and vapour pressure near the specimen (Figs. 4(c) and (d)) were simultaneously measured as well as the reference wind speed and wind direction (Figs. 4(e) and (f)). These results will be used to investigate the validity of Eq. (1) in section 5.

Errors in WDR measurements include the evaporation of adhesion water from the impervious surface of the WDR gauge and from the tube leading the collected rain water to the reservoir, and evaporation from the reservoir (Blocken and Carmeliet, 2006a). The first type of error, called the “adhesion-water evaporation error”, was estimated at only 3% for the current rain events, and therefore no correction for this was applied. The second type of error was observed to cause small decreases (0.05 mm WDR per day) of the water level in the reservoir during long drying periods. These errors were removed from the results. Another possible error is the wind error, i.e. the error introduced by the fact that the body of the WDR gauge locally changes the wind-flow pattern. This is expected to be only significant for oblique winds (Blocken and Carmeliet, 2006a). Figs. 4(e) and (f) indicate that the wind direction during the rain, for the two periods, was approximately 225°, i.e. south-west and thus perpendicular to the test facade. In addition, note that the aperture of the WDR gauge is only slightly (3 cm) protruded compared to the wall surface and therefore does not provide a large disturbance to the local wind flow pattern. For the rain events analysed in this paper, the reference wind speed is high enough (U_{10} > 2 m/s) to provide sufficient momentum to the raindrops, which are normally larger than 0.3 mm (Best, 1950). As a result, the trajectories of the larger raindrops could be assumed to follow straight lines for at least the last 3 cm to the wall, which would cause the same catch by the WDR gauge and the wall surface area. Note that smaller raindrops, which can move parallel to the wall and would not be caught by the wall, would also not be caught by the WDR gauge. Other possible errors are splashing and bouncing of raindrops at impact on the gauge collection area, but these will be discussed in the next section.

5. On the validity of the traditional approach for wind-driven rain in HAM modelling

5.1. HAM model, boundary conditions and initial conditions

In this section, the measurement data of the moisture response of the specimen to WDR are compared to the results of one-dimensional numerical HAM simulations with the traditional approach (Eq. (1)). The HAM simulations are performed with the finite element code HAMFEM (based on Compaq Visual FORTRAN 6.6), that solves the coupled equations for heat and moisture transfer in porous building materials (Janssen et al., 2007a).

The boundary conditions for heat transfer are the surface temperatures $\theta_{s,e}$ and $\theta_{s,i}$, measured at the exterior and interior surfaces of the material sample, respectively. The exterior boundary conditions for moisture transfer are the measured WDR intensity $I_{WDR,mea}$, the measured outdoor vapour pressure p_e, and the convective moisture transfer coefficient β_e. For windward facades, which are those exposed to WDR, Janssen et al. (2007b) described β_e with the following equation based on Sharples (1984) and the Lewis analogy:

$$\beta_e = 7.7 \times 10^{-9} \left(3.06 U_{10} + 5.44\right) \qquad (2)$$

For the moment, we also adopt this equation, although it clearly suffers from some limitations. For example, it does not take into account the shape and size of the building, the position at the building facade and the wind direction. At the interior surface, a zero vapour flux boundary condition is imposed, corresponding to the sealed material specimen.

For the measurements, during 20 hours before November 29, 16:00, the specimen was kept at a constant temperature of 22 ± 0.5 ºC and relative humidity of 50 ± 6 %. After that, the specimen was installed in the set-up as shown Fig. 3. So the initial temperature and moisture content of the specimen for the simulation of the first period are based on these conditions. Unfortunately the initial moisture condition of the specimen for the second period was not recorded. However, because the specimen was exposed to strong WDR intensities during 44 hours between the first and the second period, the relative humidity in the specimen is considered to have been very high at the beginning of the second period. Therefore the initial relative humidity value is set at 99 % for the simulation of the second period.

Taking into account earlier findings on the importance of the time resolution of the meteorological input data (Blocken et al. 2007), a time step of one minute was used for the simulations in this paper.

5.2. Results and discussion

5.2.1. Influence of the convective moisture transfer coefficient

Fig. 5 shows the results for the two periods and compares m_{mea} and $m_{sim}(I_{WDR,mea})$. Although there is some similarity between the curves for m_{mea} and m_{sim}, large quantitative differences are observed. The differences occur both during WDR (when large increases in weight are observed) and between separate WDR spells (i.e. the "dry" periods, when drying of the material occurs and the weight decreases). Given the accuracy of the weight change measurements, the reasons for these differences are attributed to imperfections in the model and model boundary conditions. One of the most straightforward reasons for such discrepancies is the uncertainty associated with the convective moisture transfer coefficient β_e. Janssen et al. (2007b) showed that changing β_e by a factor two can lead to changes in average moisture content in a ceramic brick wall that are larger than 100%. Therefore, in this study, simulations were also made with β_e values obtained by multiplying Eq. (2) by 2 and by dividing it by 2. Fig. 6 compares the results of simulations with the three different sets of β_e values with the measurements. Three observations are made: (1) the impact of β_e on the simulated moisture response (weight change) is very large, especially for the second period; (2) using the β_e values obtained by dividing Eq. (2) by a factor 2 provides the best "overall" agreement between m_{mea} and m_{sim} for the dry periods; (3) even with β_e from Eq.(2) / 2, large differences remain, which mainly originate during the WDR spells and which can not be attributed to the uncertainty of β_e. Fig. 6 shows that when drying behaviour is "best" taken into account by β_e in Eq. (1), m_{sim} significantly overestimates the moisture uptake m_{mea}.

The overestimation errors may be attributed to two reasons that are directly associated with the traditional approach as discussed in sections 2 and 3: (1) splashing and bouncing at raindrop impact on the material sample surface; and (2) spatial and temporal averaging of discrete and random impingement of raindrops into an average WDR flux.

5.2.2. Influence of splashing and bouncing

Due to splashing and/or bouncing of raindrops (Fig. 7), part of the raindrop volume is lost and does not contribute to the "real" moisture flux $I_{WDR,exa}$ that is available after impact for absorption and/or evaporation at the facade surface. Splashing and bouncing effects are at present not included as part of the WDR implementation in HAM models. By performing laboratory raindrop impact measurements on the surface of a dry, clean and relatively smooth ceramic brick at the terminal velocity of raindrops and at realistic impact angles, Abuku et al. (2009b) showed that splashing and bouncing can indeed occur at raindrop impact on building facades. While this study did not provide information on the fractions of the drops that are lost by splashing and bouncing, it did show that bouncing occurs on a dry ceramic brick surface for e.g. drops with diameter d = 2 mm at impact velocities around 6.8 m/s and at small impact angles ($\phi < 30°$), where the impact angle is defined as the minimum angle between the drop velocity vector and the material surface. Splashing occurs on a dry ceramic brick surface for e.g. 4 mm raindrops impacting at velocities around 7.5 m/s with impact angles $\phi > 40°$. Note that these velocities correspond to those occurring at building facades for, e.g. U_{10} = 4 and 8 m/s (Abuku et al. 2009b). In section 2, $I_{WDR,exa}$ was defined as the real exact WDR load that is supplied onto the facade material and that is available for absorption and/or evaporation. It does not include those fractions of impinging raindrops that are lost due to splashing and/or bouncing at impact. Due to splashing and bouncing, $I_{WDR,exa}$ can be different from the measured WDR load $I_{WDR,mea}$, the one determined with semi-empirical formulae $I_{WDR,sem}$ or the numerically determined one $I_{WDR,sim}$. Splashing and bouncing can indeed cause differences between $I_{WDR,exa}$ and $I_{WDR,mea}$ because these processes are likely to occur in a different way at impact on the building material surface and at impact on the WDR gauge surface. Porous building material surfaces, such as calcium silicate, but also concrete and clay brick, generally have a higher surface roughness than the impervious smooth surface of WDR gauges (PMMA, PVC, or sheet glass). Range and Feuillebois (1998) showed that the occurrence of splashing increases with increasing surface roughness. On the other hand, the presence of water drops or a water film at the impervious gauge surface and capillary action by porous materials might also influence the tendency for droplet splashing and bouncing. But, even if raindrop fractions bounce or splash back into the air after impact, they might still be retained by the bottom rim of the gauge, which has a 10 mm extension from the gauge collection area (Fig. 8). This is expected to be particularly the case at low wind speed, when the raindrop impact angle is close to vertical. Therefore, it can be argued that splashing and bouncing will cause $I_{WDR,exa}$ generally to be lower than $I_{WDR,mea}$. Note that in CFD simulations of WDR, splashing and bouncing are generally not taken into account. Therefore, assuming that the CFD simulations are accurate, $I_{WDR,sim}$ will generally be larger than $I_{WDR,exa}$. The error that is introduced in HAM simulations due to the fact that splashing and bouncing are not taken into account is called the "splashing/bouncing error."

5.2.3. Averaged flux versus discrete and random impingement of individual drops

Fig. 9 shows that the traditional approach simulates a uniform absorption and evaporation over a certain surface area, which is clearly different from the absorption and evaporation at discrete positions, resulting from the discrete and random impingement of raindrops. The use of the traditional approach, even if splashing and bouncing would be absent, could lead to a difference between m_{mea} and m_{sim}, as obtained with the traditional approach, due to differences in the absorption and evaporation processes. Abuku et al. (2009b) performed detailed HAM simulations with a "discrete" modelling approach for absorption and evaporation, in which the WDR sum was decomposed into individual drops, which were subsequently randomly distributed over the material surface. Raindrop absorption and evaporation were modelled with the finite element technique. A small part of a material surface was modelled and its volume was discretised into 10,281 finite elements. This is schematically depicted in Fig. 10. Note that, in this study, only a very small part of the material sample was modelled to limit the computational cost. The obtained results, in terms of moisture content (weight change), were compared to those obtained with the traditional approach. This numerical study showed that using an averaged WDR flux leads to an overestimation of evaporation at building facades and thus an underestimation of the moisture content/weight change of the specimen when I_{WDR} is very low (e.g. $I_{WDR} < 0.1$ mm/h under the conditions of their study); but to an underestimation of evaporation and thus an overestimation of the weight change when I_{WDR} is higher (e.g. $I_{WDR} > 0.3$ mm/h). Hence, when taking into account the fact that WDR loads with $I_{WDR} < 0.1$ mm/h only have a minor influence on the moisture content in walls (Abuku et al., 2009b), this "averaging error" will usually result in an overestimation of the average moisture content.

5.2.4. Further analysis of errors

From the above discussion, the overestimation of the moisture content/weight change obtained in this study by the application of the traditional approach in HAM modelling, cannot solely be attributed to the uncertainties in the convective moisture transfer coefficient, and may partly be attributed to the splashing/bouncing error and/or the surface averaging error. Both errors can lead to the overestimation of m_{sim} during WDR, which corresponds to the discrepancies in Fig. 6. Note that this also corresponds to the observations by Künzel and Kiessl (1997), who also found overestimations of m_{sim}.

Fig. 11(a) compares the simulated and measured material weight changes in one hour, Δm_{sim} and Δm_{mea}, during the occurrence of WDR in the two periods. In this figure, the results of the simulations with Eq. (2) / 2 for β_e are used, for which "best" results were obtained during drying periods in Fig. 6. Fig. 11(a) shows that the simulations indeed overestimate the material weight changes during WDR, and that hourly overestimations can go up to more than 100%. Note that data where $I_{WDR,mea}$ is lower than 0.1 mm/h and where Δm_{sim} and Δm_{mea} are negative (due to the low $I_{WDR,mea}$ and the high evaporation) were not included in this graph.

Fig. 11(b) shows the correlation between Δm_{sim} - Δm_{mea} for each hour and the measured wind-driven rain sum $\Delta S_{WDR,mea}$ in that hour (all for the surface area 0.25 m × 0.45 m of the specimen used in the measurements). Note that results are only shown for those hours also included in Fig. 11(a). The positive values of Δm_{sim} - Δm_{mea} indicate the overestimation of the material weight change by the simulations. A positive correlation is found, with $R^2 = 0.82$, and described by Eq. (3):

$$\Delta m_{sim} - \Delta m_{mea} = 0.34 \Delta S_{WDR,mea} \quad (3)$$

The factor 0.34 in this equation is a measure for the relative overestimation of the measurements by the simulations, i.e. the overestimation per unit of measured WDR sum. Note that this seems to correspond quite well to the reduction factor 0.7 ("rain absorptivity factor") by Künzl and Kiessl, but that a direct comparison cannot be made because it is not known if and to what extent these authors changed β_e to improve the agreement between measurements and simulations. In addition, these authors used hourly meteorological input data, while 1-minute data were used in the present study. Regardless, the argumentation in the present paper is that this factor may be related not only to errors caused by β_e, but also to errors due to splashing/bouncing and WDR flux averaging. Note that Eq. (3) was obtained for only two rain periods, and that the scatter is considerable. Therefore, this equation should not be used to correct simulation results. Instead, more research is needed on the convective moisture transfer coefficient β_e and on the quantification of the splashing/bouncing and flux averaging errors.

5.2.5. Quantification of errors

A next step in this research would be the precise quantification of the errors due to splashing/bouncing and WDR flux averaging. Concerning the splashing/bouncing error, at present, no clear information could be obtained on the fractions of the drops that splash or bounce off the facade after impact on a porous material surface. Obtaining general information on this matter is quite difficult, because these fractions do not only depend on raindrop diameter, impact speed and impact angle, but also on surface moisture content, surface roughness, etc. Concerning the averaging error, a first indication about errors was provided by Abuku et al. (2009b), in which the 1-D HAM analysis with the traditional approach overestimated the average moisture content by up to more than 200 %. Also for this error, obtaining general information is difficult, as the processes involved are quite complex and depend on a wide range of parameters. 3-D simulations of random raindrop absorption and evaporation as performed by Abuku et al. (2009b) are also very computationally expensive (more than one month using a PC with Pentium 4 of CPU = 3.0 GHz and RAM = 1 GB). The reason is that the time step has to be reduced to 10^{-5} second every time a raindrop impinges on the material surface due to a locally very high capillary pressure gradient.

As a final note, the large difference between $m_{mea}(I_{WDR,exa})$ and $m_{sim}(I_{WDR,mea})$ in this study and the discussion above seem to support at least either of these statements: (1) $I_{WDR,mea}$ is considerably higher than $I_{WDR,exa}$, which implies that either splashing and/or bouncing are considerably less pronounced on the smooth surface of the WDR gauge than on the rougher surface of the calcium silicate material sample, or the fractions of drops that splash and/or bounce off the collection area are retained by the rim of the gauge; (2) the error introduced by using the averaged WDR flux in the traditional approach is much larger

than the splashing/bouncing error in this study. In absence of further information however, neither of these statements can be definitely confirmed. Many questions on the topic of this paper remain and will need to be answered by future research.

6. Summary and conclusions

At present, numerical models for Heat-Air-Moisture (HAM) transfer in porous building materials use the traditional approach for wind-driven rain (WDR) as a boundary condition. In this traditional approach, the total mass of all raindrops impinging on a certain surface area of a building facade during the time interval of the meteorological input data is spatially and temporally averaged and is supplied to the facade as an averaged moisture flux. However, real WDR is the sum of individual raindrops that impinge on the facade in a spatially and temporally discrete modus, and that do not only spread at impact, but may also splash or bounce off the facade. Therefore, the reliability of this simplification can be questioned. This paper has presented a new experimental set-up that was developed to investigate the validity of the traditional approach under real atmospheric conditions. The set-up measures the relevant meteorological parameters, the impinging WDR intensity and the resulting material weight change of a calcium silicate building material sample. The measured WDR intensity was used to perform numerical simulations of the moisture content/material weight change with the traditional approach, and the simulation results were compared with the corresponding measurements. This comparison showed that the simulations significantly overestimated the measured average moisture content in the specimen during part of the two periods. It was shown that the uncertainty of the convective moisture transfer coefficient was not the only main source of the overestimations, because the differences between the simulated and measured responses of the sample mainly originated during WDR. The overestimations may therefore also partly be attributed to two errors that are associated with the traditional approach to implement WDR in HAM models: (1) the splashing/bouncing error and (2) the averaging error, both of which were analysed in earlier research. The splashing/bouncing error refers to the fact that fractions of raindrops that splash or bounce are not available for absorption at the facade surface. The averaging error refers to the difference in absorption and evaporation between an averaged WDR flux and a flux composed of discretely and randomly impinging drops. At this moment however, it is not possible to precisely quantify the splashing/bouncing error and the averaging error. The purpose of this paper was primarily to question the traditional approach and to point to possible error sources. Many questions on the topic of this paper remain and will need to be answered by future research. It is concluded that accurate and reliable numerical HAM simulation of the response of walls to impinging WDR is a very difficult task. Future research should quantify the influence of each of these errors on HAM analyses under real atmospheric conditions, in order to implement the insights obtained by the current study into practical models of HAM transfer under WDR loads. Finally, it is important to note that the current study focused on the moisture response of a homogeneous and isotropic building material specimen. The study did not address moisture uptake by cracks and joints, which can be dominant regarding rain penetration into building walls (e.g. Kumaran, 2003; Lacasse, 2003). Future work should also integrate this aspect to come to more comprehensive models for HAM simulations.

Acknowledgement

The results in this paper have been obtained within KUL OT/04/28, ‘Towards a reliable prediction of the moisture stress on building enclosures’, funded by the K.U.Leuven and IWT 050154, ‘Heat, air and moisture performance engineering: a whole building approach’, funded by the Flemish Government. This financial support is gratefully acknowledged.

References

Abuku, M., Blocken, B., Nore, K., Thue, J.V., Carmeliet, J., Roels, S., 2009a. On the validity of numerical wind-driven rain simulation on a rectangular low-rise building under various oblique winds. Building and Environment 44(3), 621-632.

Abuku, M., Janssen, H., Poesen, J., Roels, S. 2009b. Impact, absorption and evaporation of raindrops on building facades. Building and Environment 44(1), 113-124.

Abuku, M., Janssen, H., Roels, S., 2009c. Impact of wind-driven rain on historic brick wall buildings in a moderately cold and humid climate: numerical analyses of mould growth risk, indoor climate and energy consumption. Energy and Buildings 41(1), 101-110.

Best, A.C., 1950. The size distribution of raindrops. Quarterly Journal of the Royal Meteorological Society 76, 16-36.
Blocken, B., Carmeliet, J., 2002. Spatial and temporal distribution of wind-driven rain on low-rise building. Wind and Structures 5(5), 441-462.
Blocken, B., Carmeliet, J., 2004. A review of wind-driven rain research in building science. Journal of Wind Engineering and Industrial Aerodynamics 92(13), 1079-1130.
Blocken, B., Carmeliet, J., 2005. High-resolution wind-driven rain measurements on a low-rise building-experimental data for model development and model validation. Journal of Wind Engineering and Industrial Aerodynamics 93(12), 905-928
Blocken, B., Carmeliet, J., 2006a. On the accuracy of wind-driven rain measurements on buildings. Building and Environment 41(12), 1798-1810.
Blocken, B., Carmeliet, J., 2006b. The influence of the wind-blocking effect by a building on its wind-driven rain exposure. Journal of Wind Engineering and Industrial Aerodynamics 94(2): 101-127.
Blocken, B., Carmeliet, J., 2007. Validation of CFD simulations of wind-driven rain on a low-rise building facade. Building and Environment 42(7), 2530–2548.
Blocken, B., Roels, S., Carmeliet, J., 2007. A combined CFD-HAM approach for wind-driven rain building facades. Journal of Wind Engineering and Industrial Aerodynamics 95(7), 585-607.
Briggen P.M., Blocken B., Schellen H.L., 2009. Wind-driven rain on the facade of a monumental tower: numerical simulation, full-scale validation and sensitivity analysis, Building Environment 44(8), 1675–1690.
Choi, E.C.C., 1991. Numerical simulation of wind-driven rain falling onto a 2-D building, in: Proceedings of the Asia Pacific Conference on Computational Mechanics, Hong Kong, 1721-1728.
Choi, E.C.C., 1993. Simulation of wind-driven-rain around a building. Journal of Wind Engineering and Industrial Aerodynamics 46&47, 721-729.
Choi, E.C.C., 1994a. Determination of wind-driven rain intensity on building faces. Journal of Wind Engineering and Industrial Aerodynamics 51, 55-69.
Choi, E.C.C., 1994b. Parameters affecting the intensity of wind-driven rain on the front face of a building. Journal of Wind Engineering and Industrial Aerodynamics 53, 1-17.
Choi, E.C.C., 1999. Wind-driven rain on building faces and the driving-rain index. Journal of Wind Engineering and Industrial Aerodynamics 79(1-2), 105-122.
Dalgliesh, W.A., Surry, D., 2003. BLWT, CFD and HAM modelling vs. the real world: Bridging the gaps with full-scale measurements. Journal of Wind Engineering and Industrial Aerodynamics 91(12-15), 1651-1669.
Hall, C., Kalimeris, A.N., 1982. Water movement in porous building materials–V. Absorption and shedding of rain by building surfaces. Building and Environment 19, 13-20.
Hall, C., Kalimeris, A.N., 1984. Rain absorption and run-off on porous building surfaces. Canadian Journal of Civil Engineering 11, 108-111.
Hagentoft, C.-E., Kalagasidis, A.S., Adl-Zarrabi, B., Roels, S., Carmeliet, J., Hens, H., Grune-wald, J., Funk, M., Becker, R., Shamir, D., Adan, O., Brocken, H., Kumaran, K., Djebbar, R., 2004. Assessment method of numerical prediction models for combined heat, air and moisture transfer in building components: benchmarks for one-dimensional cases. Journal of thermal envelope and building science 27(4), 327-352.
Hangan, H., 1999. Wind-driven rain studies. A C-FD-E approach. Journal of Wind Engineering and Industrial Aerodynamics 81(1-3), 323-331.
Hens, H., Janssens, A., Zheng, R., 2003. Zinc roofs: an evaluation based on test house measurements. Building and Environment 38(6), 795-806.
Högberg, A.B., Kragh, M.K., van Mook, F.J.R., 1999. A comparison of driving rain measurements with different gauges, in: Proceedings of the 5th Symposium on Building Physics in the Nordic Countries, Gothenburg, Sweden, 361-368.
Janssen, H., Blocken, B., Carmeliet, J., 2007a. Conservative modelling of the moisture and heat transfer in building components under atmospheric excitation. International Journal of Heat and Mass Transfer 50, 1128-1140.
Janssen, H., Blocken, B., Roels, S., Carmeliet, J., 2007b. Wind-driven rain as a boundary condition for HAM simulations: analysis of simplified modelling approaches. Building and Environment 42, 1555-1567.
Karagiozis, A.N., Salonvaara, M., Holm, A., Kuenzel, H., 2003. Influence of wind-driven rain data on hygrothermal performance, in: Proceedings of the Eighth International IBPSA Conference, Eindhoven, the Netherlands, 627-634.

Kumaran M.K., 2003. HAM activities at the Institute for Research in Construction since Hamtie Annex 24. IEA Annex 41 Whole Building Heat, Air and Moisture Response, International Report A41-T0-C-03-2.
Künzel, H.M., Kiessl, K., 1997. Calculation of heat and moisture transfer in exposed building components. International Journal of Heat and Mass Transfer 40(1), 159-167.
Lacasse, M.A., 2003. Recent studies on the control of rain penetration in exterior wood-frame walls. BSI 2003 Proceedings, October 2003, p. 1-6. (http://irc.nrc-cnrc.gc.ca/fulltext/nrcc46889/)
Range, K., Feuillebois, F., 1998. Influence of surface roughness on liquid drop impact. Journal of Colloid and Interface Science 203(1), 16-30.
Roels, S., Carmeliet, J., Hens, H., Adan, O., Brocken, H., Cerny, R., Pavlik, Z., Hall, H., Kumaran, K., Pel, L., Plagge, R., 2004. Interlaboratory comparison of hygric properties of porous building materials. Journal of thermal envelope and building science 27(4), 307-325.
Sanders, C., 1996. Heat, air and moisture transfer in insulated envelope parts. IEA Annex 24, Final report – Vol. 2, Task 2: Environmental conditions. Acco Leuven, Leuven, Belgium.
Sharples, S., 1984. Full scale measurements of convective energy losses from exterior building surfaces. Building and Environment 19, 31-39.
Straube, J., Schumacher, C., 2006. Assessing the durability impacts of energy efficient enclosure upgrades using hygrothermal modeling. WTA-Journal 2006, 2/06, 197-222
Tang, W., Davidson, C.I., Finger, S., Vance, K., 2004. Erosion of limestone building surfaces caused by wind-driven rain. 1. Field measurements. Atmospheric Environment 38(33), 5589-5599.
Tang, W., Davidson, C.I., 2004. Erosion of limestone building surfaces caused by wind-driven rain. 2. Numerical modelling. Atmospheric Environment 38(33), 5601-5609.
van Mook, F.J.R., 2002. Driving rain on building envelopes, PhD thesis, Building Physics Group (FAGO), Eindhoven University of Technology, Eindhoven University Press, Eindhoven, the Netherlands.

Figure and Table captions

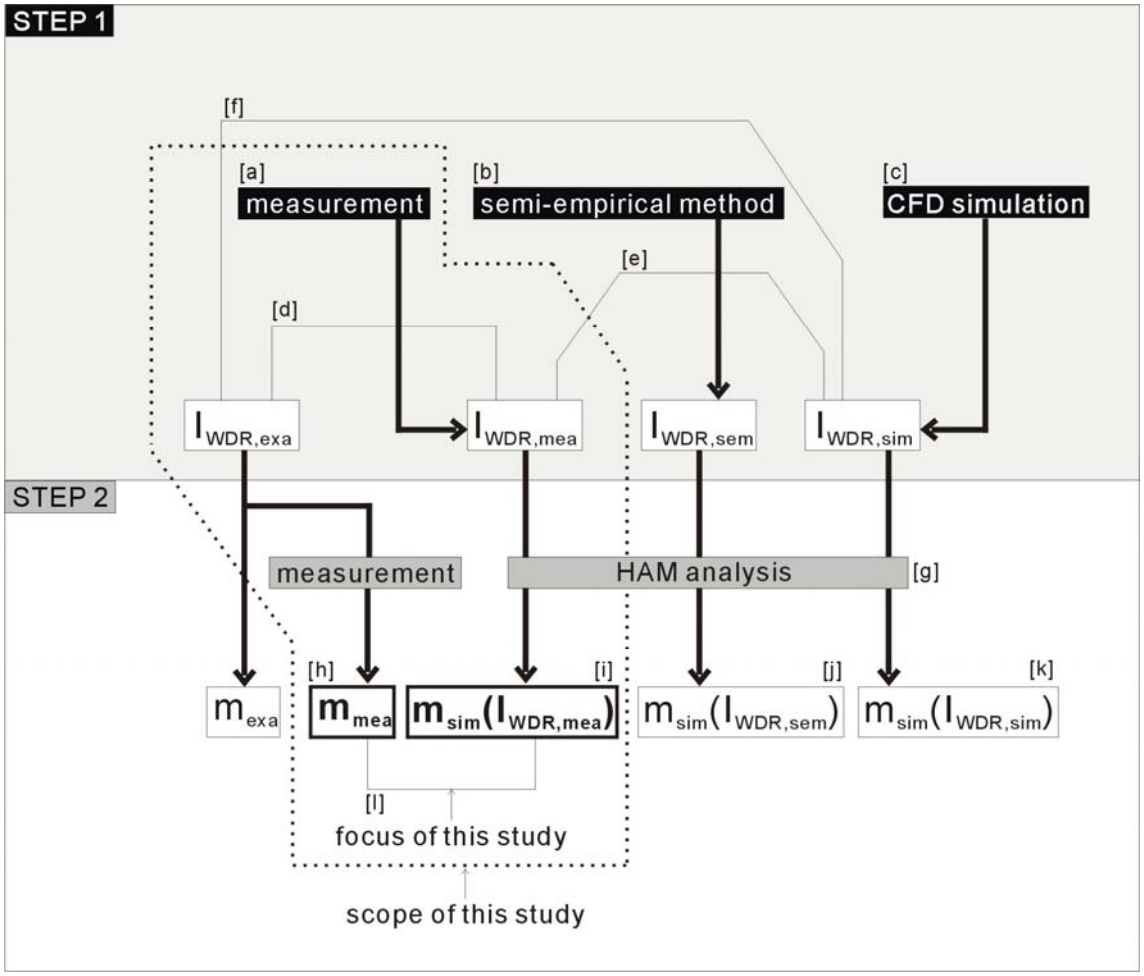

Fig. 1. Recent studies and the scope and focus of the current study in approaches to determine (step 1) wind-driven rain (WDR) loads and (step 2) the response of walls to WDR. I_{WDR}: wind-driven rain intensity (mm/h); *m*: weight change of a specimen (g). For subscripts, *exa* represents the exact value; *mea* the measured one; s*em* the one calculated by a semi-empirical formula; *sim* the numerically simulated one. $I_{WDR,exa}$ is the real exact WDR load that is supplied onto the facade material and that is available for absorption and/or evaporation. It does not include those fractions of impinging raindrops that are lost due to splashing and bouncing at impact. Note that although only wind-driven rain and the response of walls to it are considered here for simplicity, other boundary conditions and material properties are also needed as input for step 2. The letter labels [a] – [l] correspond to the entries in Table 1.

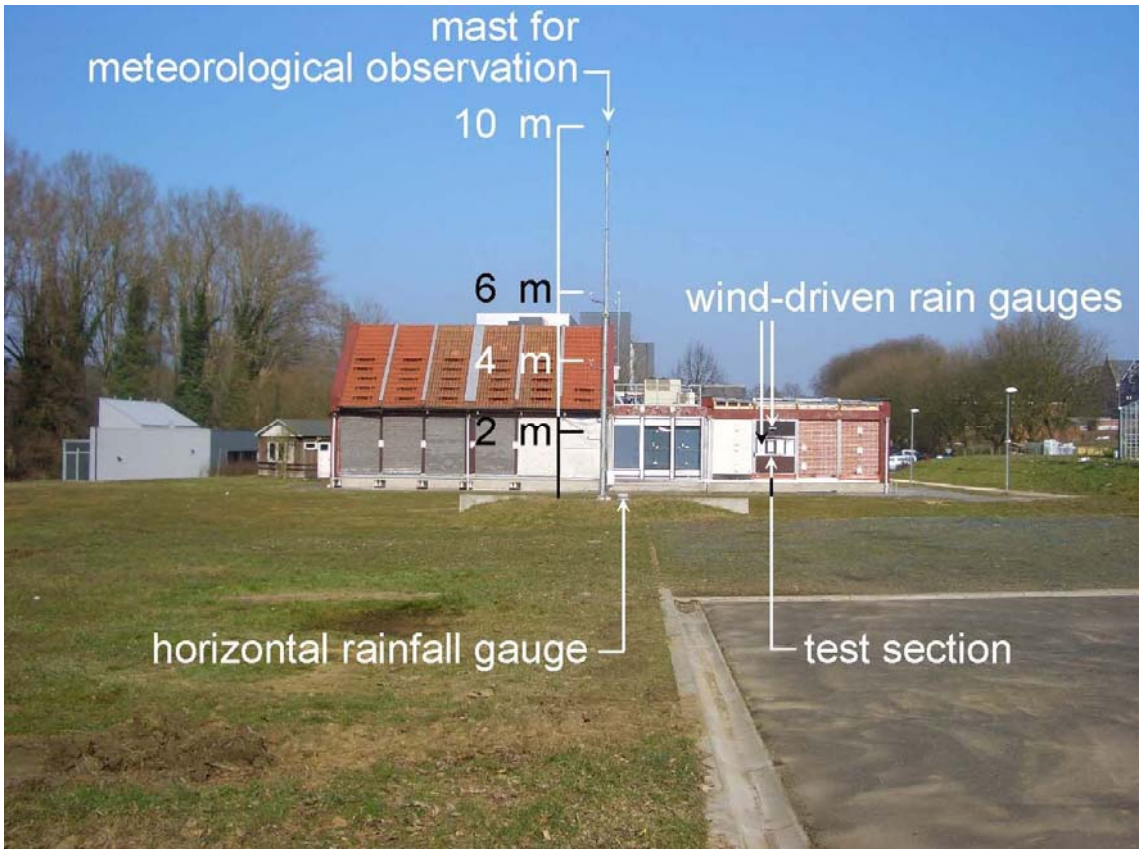

Fig. 2. VLIET test building and the surrounding environment (view from south-west). The meteorological mast with anemometers at different altitudes, the position of the horizontal rainfall gauge, the test section and some of the wind-driven rain gauges are also indicated.

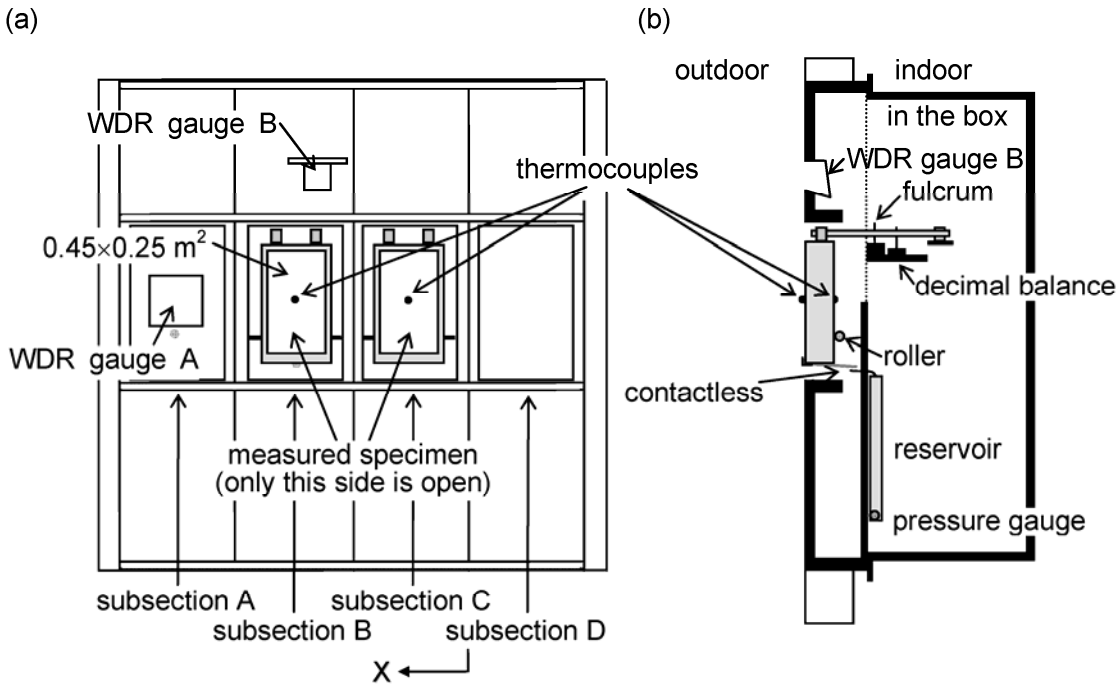

Fig. 3. Schematic diagram of the test section and the new set-up at the south-west facade. (a) Elevation and (b) X-intersection.

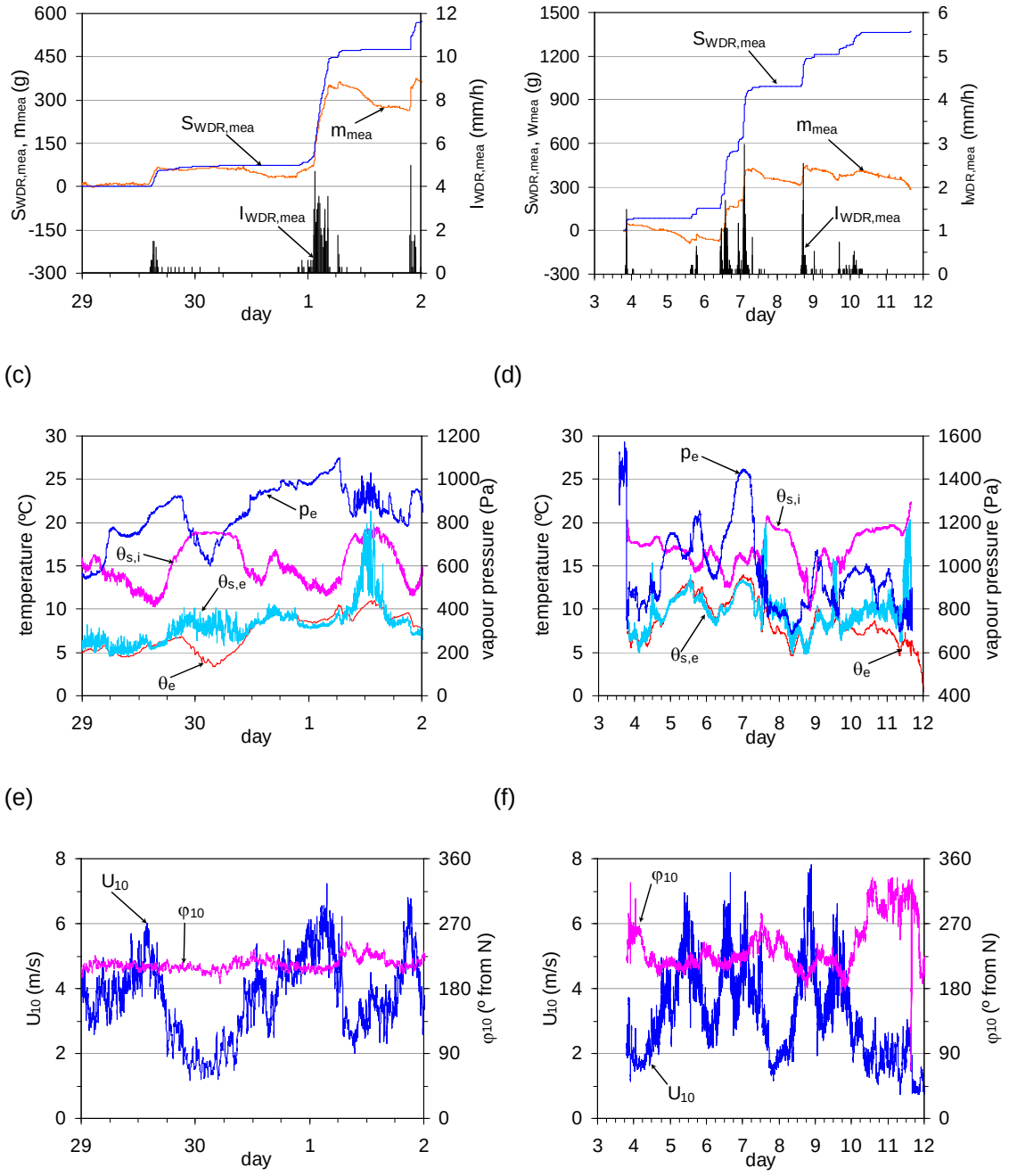

Fig. 4. Measurement results of (a,c,e) November 29 - December 2, 2007 and (b,d,f) December 3 -12, 2007. (a,b) weight change of the specimen m_{mea}, cumulative amount $S_{WDR,mea}$ and intensity $I_{WDR,mea}$ of wind-driven rain; (c,d) outdoor temperature θ_e, outdoor vapour pressure p_e, and temperatures at the inside and outside material surfaces $\theta_{s,e}$ and $\theta_{s,i}$; (e,f) wind speed U_{10} and wind direction φ_{10} (10 m above the ground level). φ_{10} is given in degrees from north.

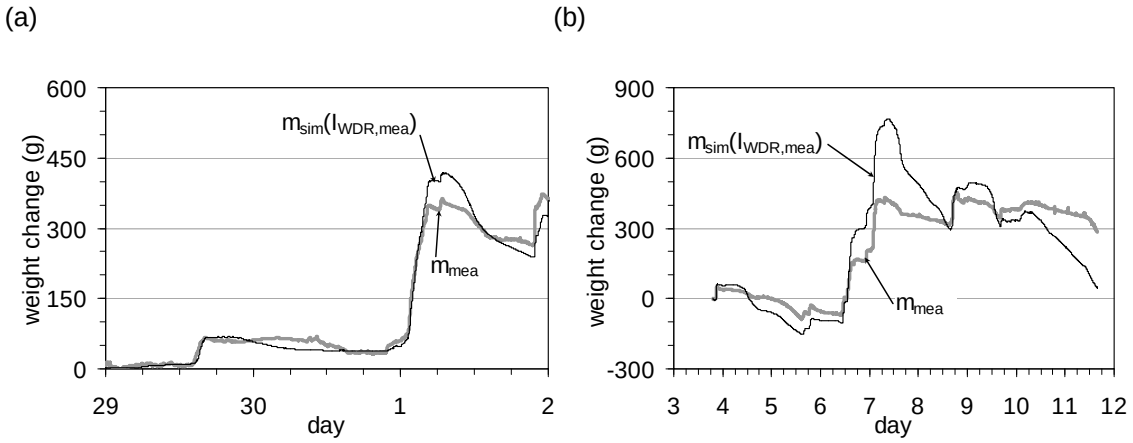

Fig. 5. Simulated weight changes $m_{sim}(I_{WDR,mea})$ of the specimen compared to measured ones m_{mea} for the two periods. (a) 29/11/2007 - 2/12/2007 and (b) 3/12/2007 - 12/12/2007.

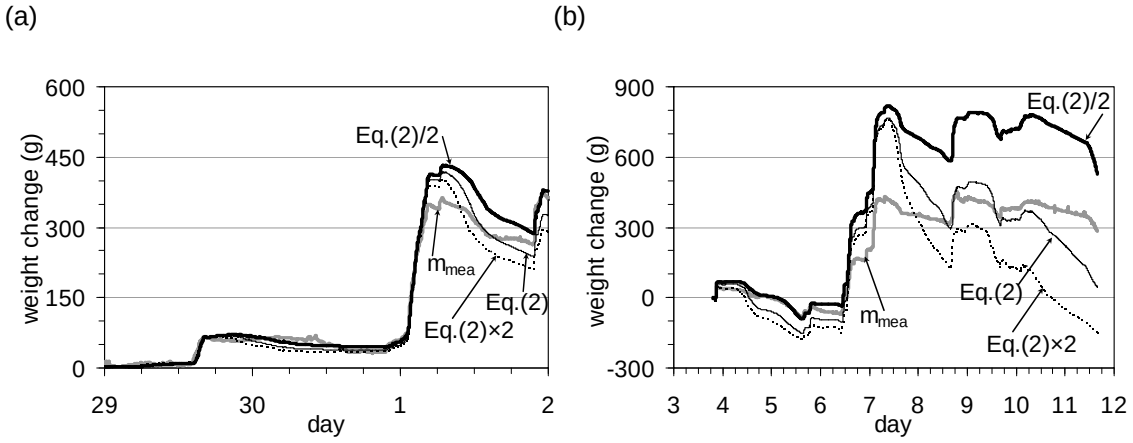

Fig. 6. Influence of the convective moisture transfer coefficient on simulation results for the two periods. (a) 29/11/2007 - 2/12/2007 and (b) 3/12/2007 - 12/12/2007.

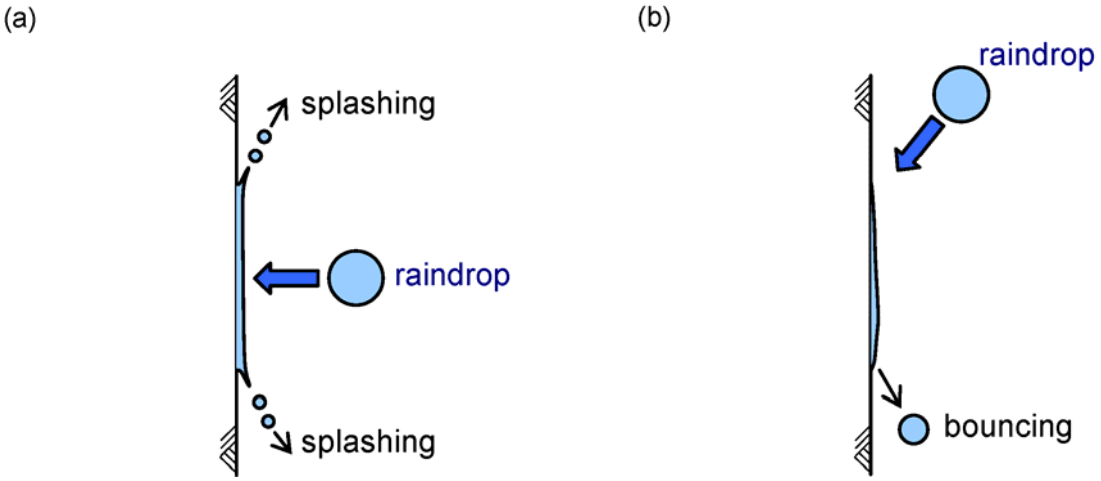

Fig. 7. (a) Splashing and (b) bouncing at raindrop impact on a vertical surface.

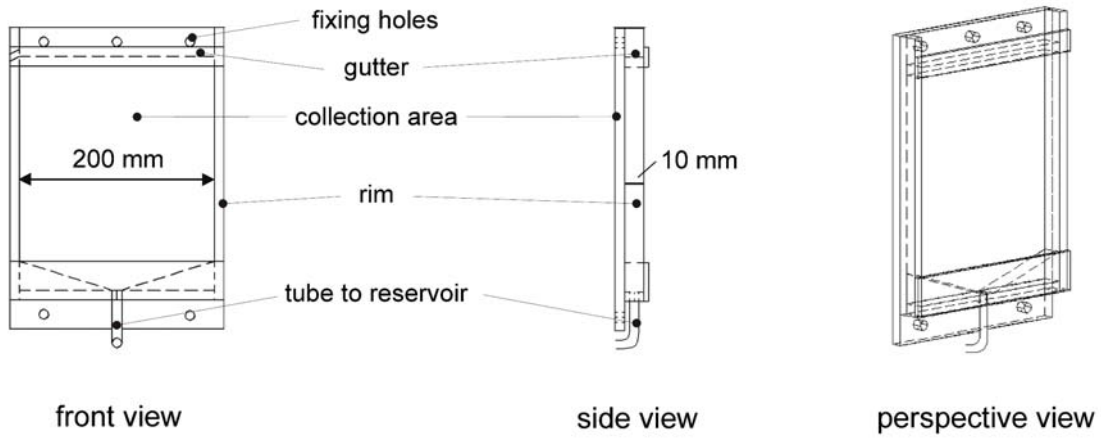

Fig. 8. Wall-mounted wind-driven rain gauge used in this study and in earlier studies (Blocken and Carmeliet 2005, 2006a). The gauge is made of PMMA (polymethyl-methacrylate) with a collection area of 0.2 × 0.2 m².

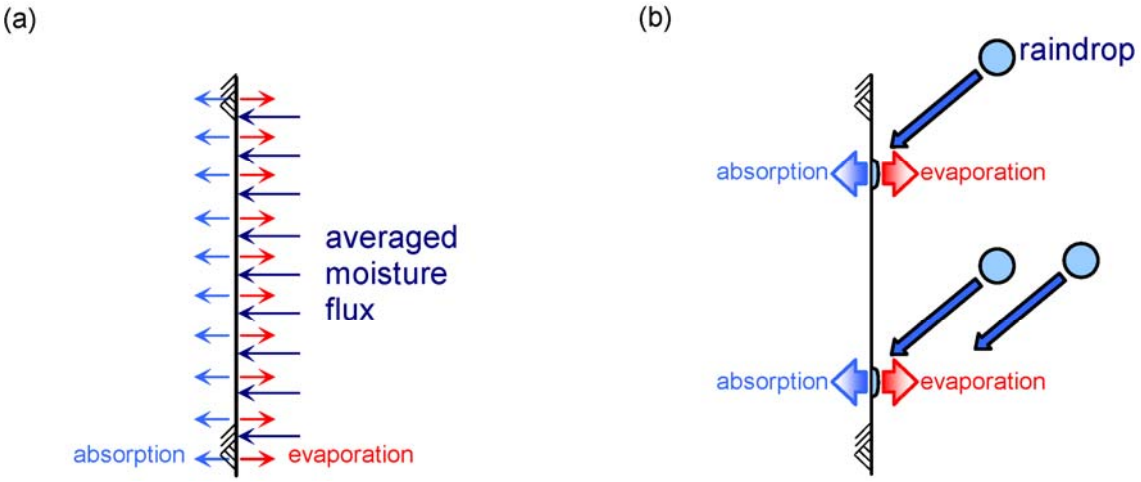

Fig. 9. (a) Averaged flux assumption, resulting in uniform absorption and evaporation over a given surface area, versus (b) the reality of discretely and randomly impinging drops, resulting in absorption and evaporation at discrete positions.

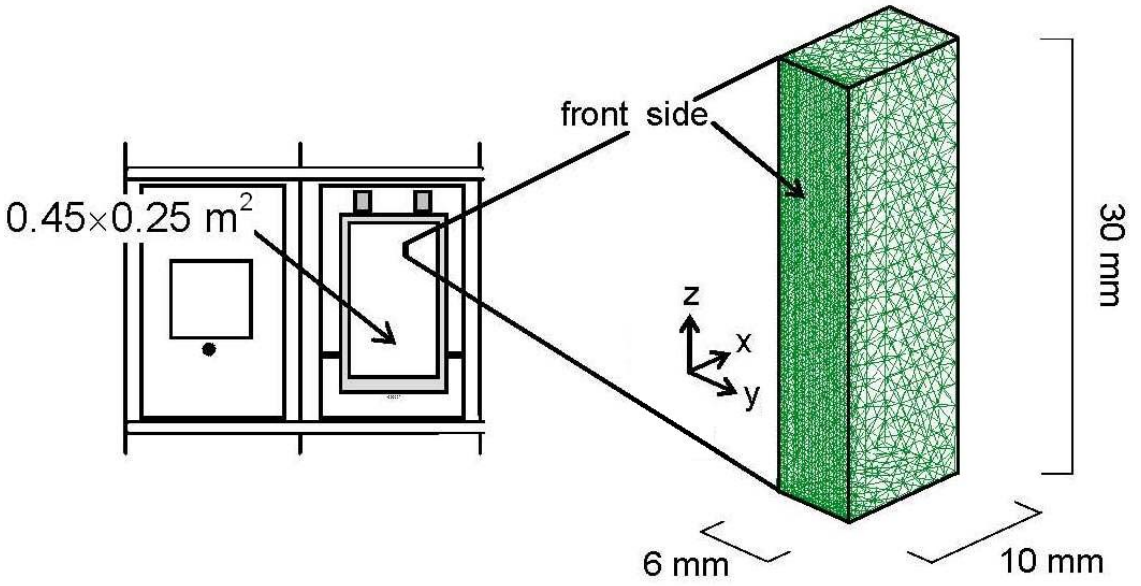

Fig. 10. (a) Material sample at test section B; (b) Finite element mesh of part of this sample, generated for the three-dimensional analysis of absorption and evaporation of raindrops after impact at the building facade (Abuku et al., 2009b).

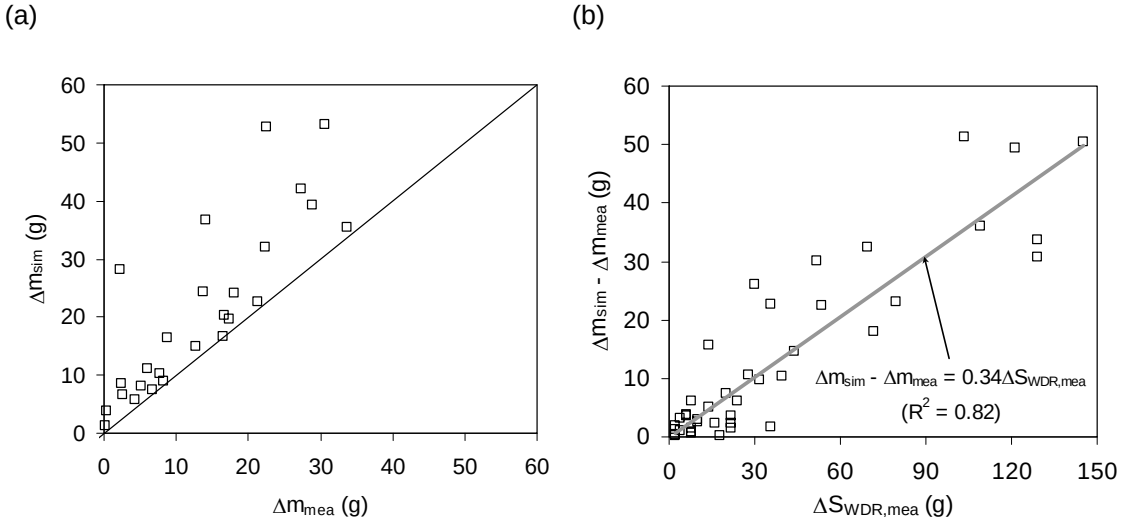

Fig. 11. (a) Comparison of Δm_{sim} and Δm_{mea}. (b) Correlation between Δm_{sim} - Δm_{mea} and $\Delta S_{WDR,mea}$. Δm_{sim} and Δm_{mea}: simulated and measured material weight changes in one hour (g), respectively; $\Delta S_{WDR,mea}$: measured wind-driven rain sum in one hour (calculated for the surface area 0.25 m × 0.45 m of the specimen used in the measurements) (g).

Table 1. Focus of past wind-driven rain (WDR) research shown in Fig. 1.

Step	[a] – [l] in Fig.1	Focus	Reference
1	[a]	quantification of WDR intensity $I_{WDR,mea}$ by measurements	reviewed in Blocken and Carmeliet (2004)
	[b]	determination of parameters to establish semi-empirical formula to quantify WDR intensity $I_{WDR,sem}$	e.g. Sanders (1996); also reviewed in Blocken and Carmeliet (2004)
	[c]	numerical modelling of airflow field and raindrop trajectories (CFD WDR simulation) to quantify WDR intensity $I_{WDR,sim}$	e.g. Choi (1993); Blocken and Carmeliet (2002); also reviewed in Blocken and Carmeliet (2004)
	[d]	error estimate in WDR measurements	e.g. Högberg et al. (1999); Van Mook (2002); Blocken and Carmeliet (2005, 2006a)
	[e]	comparison of $I_{WDR,sim}$ and $I_{WDR,mea}$	Hangan (1999); Van Mook (2002); Blocken and Carmeliet (2002, 2006b, 2007); Tang and Davidson (2004); Tang et al. (2004); Abuku et al. (2009a); Briggen et al. (2009)
	[f]	spreading, splashing and bouncing of raindrops at building facades	Abuku et al. (2009b)
2	[g]	numerical modelling for the hygrothermal analysis of building enclosures	e.g. Hall and Kalimeris (1982, 1984); Künzel and Kiessl (1997); Hagentoft et al. (2004); Abuku et al. (2009b)
	[h]	field measurement of hygrothermal response (m_{mea}) of building facades to $I_{WDR,exa}$	Künzel and Kiessl (1997)
	[i]	numerical analyses of hygrothermal response ($m_{sim}(I_{WDR,mea})$) of building facades to $I_{WDR,mea}$	e.g. Künzel and Kiessl (1997)
	[j]	numerical analyses of hygrothermal response ($m_{sim}(I_{WDR,sem})$) of building facades to $I_{WDR,sem}$	e.g. Karagiozis et al. (2003); Straube and Schumacher (2006)
	[k]	numerical analyses of hygrothermal response ($m_{sim}(I_{WDR,sim})$) of building facades to $I_{WDR,sim}$	Blocken et al. (2007); Janssen et al. (2007a, 2007b); Abuku et al. (2009b, 2009c)
	[l]	comparison of m_{mea} and $m_{sim}(I_{WDR,mea})$*	Künzel and Kiessl (1997); present study

* Künzel and Kiessl (1997) determined $m_{sim}(I_{WDR,mea})$ by adjusting a (global) rain absorptivity (for the entire measurement period of 80 days), i.e. the ratio of rain absorption rate per unit surface area to $I_{WDR,mea}$.